Research Article | Vol. 31, No. 20 / 25 Sep 2023 / *Optics Express* 32813

Optics EXPRESS

High power optical frequency comb with 10^{-19} frequency instability

XIAODONG SHAO,[1] HAINIAN HAN,[1,2,*] HUIBO WANG,[1] JUNYI MA,[1] YUE HU,[2] CHENGZHI LI,[1] HAO TENG,[1] GUOQING CHANG,[1] BINGBING WANG,[1] AND ZHIYI WEI[1,2,3]

[1] *Beijing National Laboratory for Condensed Matter Physics, Institute of Physics, Chinese Academy of Sciences, Beijing 100190, China*
[2] *Songshan Lake Materials Laboratory, Dongguan, Guangdong 523808, China*
[3] *zywei@iphy.ac.cn*
[*] *hnhan@iphy.ac.cn*

Abstract: Optical frequency combs with more than 10 W have paved the way for extreme ultraviolet combs generation by interaction with inert gases, leading to extreme nonlinear spectroscopy and the ultraviolet nuclear clock. Recently, the demand for an ultra-long-distance time and frequency space transfer via optical dual-comb proposes a new challenge for high power frequency comb in respect of power scaling and optical frequency stability. Here we present a frequency comb based on fiber chirped pulse amplification (CPA), which can offer more than 20 W output power. We further characterize the amplifier branch noise contribution by comparing two methods of locking to an optical reference and measure the out-of-loop frequency instability by heterodyning two identical high-power combs. Thanks to the low noise CPA, reasonable locking method, and optical path-controlled amplifiers, the out-of-loop beat note between two combs demonstrates the unprecedented frequency stability of 4.35×10^{-17} at 1s and 6.54×10^{-19} at 1000 s.

1. Introduction

Optical frequency combs (OFCs) have enabled the landmarked progress of optical atomic clocks [1–3], and expanded increasingly to various applications, such as attosecond science [4], fundamental constants measurement [5], length measurement [6], Earth-like planet detection [7], dual-comb molecule spectroscopy [8], microwave photonics [3,9], and time-frequency transfer [10–12] over the last two decades. Although these applications inversely enhanced the OFCs technology, few results were reported regarding fully stabilized high-power OFCs with ultrahigh in-loop frequency stability better than 10^{-18} at 1s. Based on the frequency stability transmission characteristics of OFC, it is possible to generate an ultraviolet comb with the same frequency stability as a near-infrared high-power comb through high-order harmonic generation technology. This is of significant importance for precision ultraviolet spectroscopy [13] and nuclear atomic clocks [14]. But there are two main problems for achieving both high power and high stability. One is how to realize low phase noise power amplification with dependable carrier-envelope phase offset (CEO) stabilization and the other is how to phase-lock the comb teeth directly to an ultrastable continuous wave (CW) laser with a broad bandwidth feedback system. For the first problem, Ytterbium (Yb) doped fiber laser is attractive for power scaling [15] by using large-mode-area (LMA) Yb-doped photonic crystal fiber (PCF). Due to the larger mode field area and "endlessly single-mode" behavior [16], it is beneficial to reduce the nonlinear effect in the amplification and easy to obtain single-mode and low-noise femtosecond laser output [17]. With the LMA Yb-PCF, the average power of the optical comb has further increased to more than 100 W [18–21]. In a recent report, the CEO stabilized Yb-fiber chirped-pulse amplification (CPA)

#499383 https://doi.org/10.1364/OE.499383
Journal © 2023 Received 11 Jul 2023; revised 15 Aug 2023; accepted 16 Aug 2023; published 18 Sep 2023

Optics EXPRESS

system based on a coherent beam combination technique [22] was up to 1 kW of average power [23]. However, none of the above-mentioned has proved the ultrahigh frequency stability of the OFC teeth, which is especially necessary for such applications as low noise microwave frequency generation [9], time-frequency transfer [10], and the comparison of optical clock networks [24]. To some extent, the challenge of locking the high power comb to the ultrastable CW laser with 10^{-18} at 1 s in-loop instability would be more difficult regarding the precision locking technique with broad bandwidth and extreme robustness. In 2008, JILA and IMRA demonstrated a 10 W OFC with 1 mHz linewidth by using a fast piezoelectric transducer (PZT) for feedback [25]. In 2012, they reported a novel extreme ultraviolet frequency comb generation driven by an 80 W frequency comb which is stabilized to an iodine-stabilized Nd:YAG laser in the same way [13]. But the bandwidth of the PZT is typically limited to a few kHz-level, which restricts the available stability of the comb. Though several techniques have been considered to broaden the servo bandwidth [26,27], using an electro-optic modulator (EOM) to modulate the phase of the intracavity laser is not only able to provide faster processing speed with less than µs response time to efficiently suppress the high frequency noise [28] but also favorable for the robust nonlinear polarization evolution (NPE) operation and long-term stabilization.

Two further concerns for high power combs are how to lock the comb to CW laser and how to measure the out-of-loop instability. Firstly, there are two ways of locking the OFC to the optical reference. One is directly locking the oscillator output to the optical reference, the other is locking the amplifier output to the optical reference. In an amplifier, the amplified spontaneous emission (ASE) [29], nonlinear phase shift during fiber amplification [17], and spectral coherence deterioration in supercontinuum generation [30] will produce high-frequency additive noise in the range of higher than kHz [31]. Meanwhile, the environmental fluctuation induces parametric noise in the low-frequency range lower than 1 kHz [32,33], due to the tens of meters of the non-common-mode optical path in the fiber amplifier. Thus, these two locking methods would have significantly different impacts on the stability of the high power comb. The comparison of these two locking methods would reveal the quantitative noise contributions in the high power amplifier. However, this work has not been reported today.

Though the in-loop frequency instability has been demonstrated to be 10^{-18} or even 10^{-19} at 1 s averaging time in much low-power fiber-based comb systems, it mainly shows the tracking performance of the optical phase-locked loop (PLL). Only the out-of-loop frequency instability can faithfully reflect the actual performance of the comb [34]. At present, the out-of-loop frequency instability of the combs without noise cancellation is worse than 10^{-16}/s, which is limited by the non-common mode path noise from the in-loop locking point to the out-of-loop measuring point [35–38]. Here, instead of using a complex noise cancellation setup, we further improve the out-of-loop stability to 10^{-17}/s level by reasonably designing the amplifier structure to make the out-of-loop measuring point as close as possible to the in-loop locking point.

In this study, we demonstrate a high average power and high-frequency stability Yb-fiber OFC achieved by the LMA Yb-PCF and CPA technique. The single-mode and low-noise femtosecond laser pulse output with power over 20 W and duration of 75 fs at the repetition rate of 200 MHz is obtained, whose time-frequency transform is close to the limit of Fourier transform. With an EOM inserted in the NPE mode-locked Yb-fiber oscillator, the comb is locked to an ultrastable CW laser at 1064 nm. The CEO signal is locked directly to a microwave reference and the stability of 2.4×10^{-19} at 1000 s at the optical carrier frequency is gotten. Moreover, to investigate deeply the stability characteristics of the high power comb, we compared the frequency instability and the noise power spectral density (PSD) of the 20 W output between the two locking methods. The experimental results show that when the oscillator branch or the amplifier branch is locked to the optical reference, the instability of the 20 W output is 2.7×10^{-16} and 2.8×10^{-20} in 1000 s, respectively, with four orders of magnitude difference. It indicates that the non-common-mode optical path between the oscillator and amplifier will induce a lot of low-frequency differential

Optics EXPRESS

noise, which can be well suppressed by locking the amplifier branch to the optical reference. After the comprehensive characterization and optimization of the high-power optical combs, we measured the out-of-loop frequency instability between two identical high power combs. The frequency instability of out-of-loop beat note reaches an unprecedented 4.35×10^{-17} at 1 s and 6.54×10^{-19} at 1000 s.

2. High power frequency comb with f_{ceo} locked

Figure 1 shows the configuration of the high power fiber comb, which consists of a mode-locked fiber seed source, a fiber CPA, and a comb-locking module. The seed source based on NPE mode-locking [39] is a homemade Yb-fiber oscillator, with a 56 nm spectral bandwidth centered around 1030 nm. The net dispersion of the oscillator is close to zero for operation in the stretched-pulse regime and to obtain the narrowest f_{ceo} signal [40]. The oscillator spectrum is shown by the black line in Fig. 2(a). The repetition rate is about 200 MHz, with a tuning range of 6 MHz by installing a 25 mm travel translation stage under the end mirror. To lock the OFC to the optical reference, the Yb: fiber oscillator is equipped with a 2 mm × 2 mm × 7 mm EOM in the cavity and a PZT on one of the cavity mirrors [41]. The oscillator is housed in a double-layer aluminum box with thermal insulation and vibration isolation, and the thermoelectric coolers (TECs) are placed underneath the inner aluminum box.

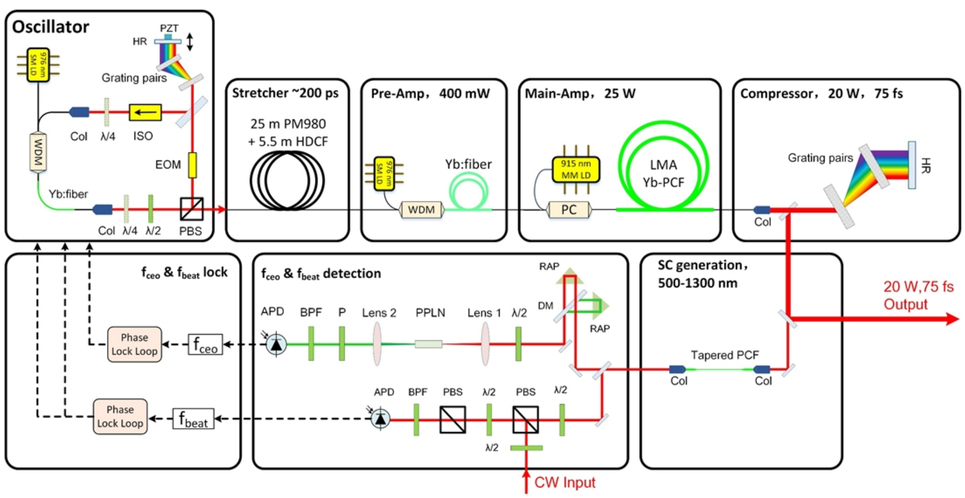

Fig. 1. Experimental setup. ISO: isolator, λ/4: quarter-wavelength plate, λ/2: half-wavelength plate, Col: collimator, EOM: electro-optic modulator, PBS: polarizing beam splitter, WDM: wavelength division multiplexer, HR: high reflection mirror, PZT: piezo-electric transducer, PM980: polarization maintaining fiber, HDCF: High-order dispersion compensation fiber, SM LD: single-mode laser diode, PC: pump combiner, MM LD: multimode laser diode, Tapered PCF: tapered photonic crystal fiber, RAP: right-angle prism mirror, DM: dichroic mirror, PPLN: periodically poled lithium niobate, P: film polarizers, BPF: bandpass filter, APD: avalanche photodetector, f_{ceo}: carrier-envelope offset. Black solid line: passive fiber, Green solid line: gain fiber or PCF, Red solid line: optical path, Black dashed line: electronic wire.

The oscillator emits up to 60 mW of average power, which is coupled to a single-mode polarization-maintaining fiber and split by a fiber power splitter to two-part, 90% for amplification, and 10% for repetition rate and spectral monitoring. In the stretcher part, a 25 m single-mode polarization-maintaining fiber (PM980) and a 6 m high-order dispersion compensation fiber (HDCF) are used to broaden the pulse width to 200 ps. The third-order dispersion of HDCF is

Optics EXPRESS

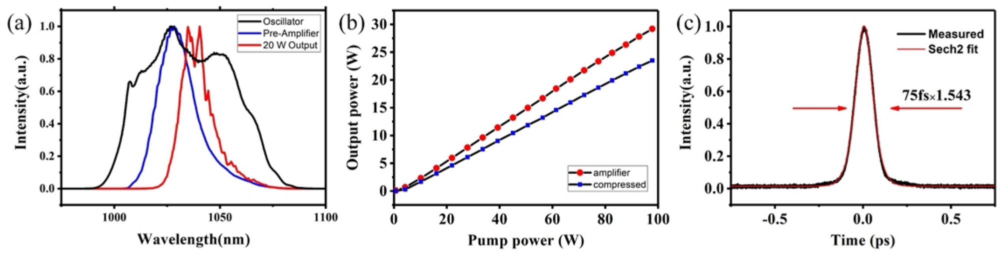

Fig. 2. (a) The output spectrum of the oscillator (black line), pre-amplifier (blue line), and main amplifier (red line). (b) The output power of the main amplifier (red dot line) and grating pairs compressor (blue dot line) versus pump power. (c) Temporal properties of the output of the main amplifier and sech2 fitting after grating pairs compressor.

negative in the 1 μm wavelength region, which can be used to manage the high-order dispersion of the CPA part. Due to the large splicing loss of HDCF where every fusion point is 2.5 dB, the output power after the stretcher is about 14 mW. One stage single-mode polarization-maintaining Yb-doped fiber amplifier is used as a pre-amplifier to increase the input power with low noise. The gain fiber of the pre-amplifier is 70 cm Yb401-PM. The output power is boosted to about 400 mW when pumped with about 600 mW at 976 nm. The pre-amplifier spectrum is shown by the blue line in Fig. 2(a).

A 5-meter LMA Yb-PCF (DC-200/40-PZ-Yb) is used as the gain fiber of the main amplifier. The LMA fiber can effectively alleviate the nonlinear effect in the amplification process and avoid nonlinear phase shifts in the fiber propagation. Two laser diodes (LDs) at 915 nm are used as the pump laser with a maximum total output power of 140 W. Although the 976 nm LD has higher pumping efficiency, the sharp absorption peak at 976 nm makes Yb-doped fiber more sensitive to the wavelength shift of LD. The broadband absorption spectrum at 915 nm reduces the influence of LD frequency shift, which makes the intensity noise lower and suppresses the conversion from intensity noise to phase noise [19]. When the pump power is 97.8 W, the output power is 29.19 W and the amplifier efficiency is 30% as described in Fig. 2(b). The output spectrum after amplification is shown by the red line in Fig. 2(a), with a central wavelength of 1037 nm and an FWHM of 17 nm.

The pulses are compressed by a pair of 1000 lines/mm transmission grating. By carefully optimizing the spacing of the grating compressor and the length of the stretcher fiber, the second-order dispersion and the third-order dispersion can be adjusted to zero simultaneously to obtain the best compression effect. Finally, when the grating compressor spacing is 23 cm, the pulse width of 75 fs and the power of 23.5 W is obtained. The characteristics of power and pulse duration are shown in Fig. 2(b) and Fig. 2(c). The grating pairs' compression efficiency is 80%. In Fig. 2(c), the compressed pulse has almost no wing structures, which indicates that the higher-order dispersion of this laser has been well compensated and the B-integral is estimated to be 0.2.

To achieve precise phase control, a piece of tapered PCF with a zero-dispersion wavelength of 1000 nm is employed to generate the supercontinuum spectrum. The length of the cone of tapered PCF is about 6 cm, and the total length is 15 cm. In the case of an injection power of 200 mW, the output power behind the PCF is 80 mW and a spectrum covering one octave is generated, as shown in the inset of Fig. 3(a). A standard f-2f interferometer is built for the carrier envelope offset f_{ceo} signal detection. The signal-to-noise ratio (SNR) of the f_{ceo} signal is 37 dB at 300 kHz resolution bandwidth (RBW), shown in Fig. 3(a). To stabilize the f_{ceo} signal, the pump current of the oscillator is controlled by a phase-locked loop circuit. The inset of Fig. 3(b) shows the frequency count of the locked f_{ceo} signal in 3 hours, with a standard deviation of 4.04 mHz. The

Optics EXPRESS

modified Allan Deviation instability, shown in Fig. 3(b), is 1.4×10^{-17} at 1 s gate time and drops to 2.9×10^{-19} at 1000 s.

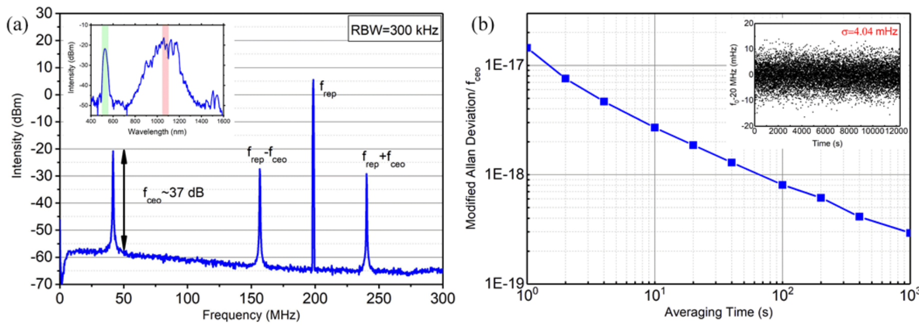

Fig. 3. (a) Radio-frequency spectrum of f_{ceo} and f_{rep}. The inset: supercontinuum spectrum. (b) Modified Allan Deviation of f_{ceo}. The inset: the frequency fluctuations of the locked f_{ceo} signal for about 12000 s recorded by the counter at 1 s gate time.

3. Instability measurements and discussion

3.1. Oscillator branch and amplifier branch instability comparison

To evaluate the noise contributions in the amplifier, two heterodyne beam paths were built to compare the oscillator branch locked to optical reference and the amplifier branch locked to optical reference as illustrated in Fig. 4(a). A 1064 nm ultrastable CW laser was employed as the optical reference. The CW laser is stabilized on a high-finesse Fabry-Perot cavity using PDH technology. The beat note between the oscillator output and the optical reference is denoted as $f_{\mathrm{b,osc}}$; the beat note between the output after the amplifier and supercontinuum generation and the optical reference is denoted as $f_{\mathrm{b,amp}}$. The SNR of the two beat notes is about 40 dB as shown in Fig. 4(b) with 300 kHz RBW. To realize the high stability of the beat notes, we used a broadband response bandwidth EOM as fast loop control and a PZT as slow loop control. These two beat notes are locked by controlling the PZT and EOM of the oscillator by a phase-locked loop circuit separately. Then, we performed frequency countings and phase noise analysis on the beat notes $f_{\mathrm{b,osc}}$ and $f_{\mathrm{b,amp}}$ simultaneously. Since we only explored the noise characteristics of a specific comb line in different branches, f_{ceo} was not locked in both branches. This also avoids the crosstalk caused by the simultaneous locking of f_{ceo} and f_{beat} [31,42]. Figure 4(c) shows the RF spectra of the two beat notes when the $f_{\mathrm{b,osc}}$ is locked and the $f_{\mathrm{b,amp}}$ is unlocked. The SNR of coherent carriers of two beat notes exceeds 50 dB, and the noise of both beat notes is suppressed. Conversely, if $f_{\mathrm{b,amp}}$ is locked and $f_{\mathrm{b,osc}}$ is unlocked, which has similar RF spectra.

The frequency instability of the amplifier branch with a high average power of 20 W is mainly concerned with applications. Thus the phase noise and modified Allan deviation of $f_{\mathrm{b,amp}}$ in different locked states are depicted in Fig. 5. In Fig. 5(a), the blue line is the phase noise measured when $f_{\mathrm{b,osc}}$ is locked, and $f_{\mathrm{b,amp}}$ is unlocked. The red line is the phase noise measured when $f_{\mathrm{b,amp}}$ is locked, but $f_{\mathrm{b,osc}}$ is unlocked. The dashed lines in Fig. 5(a) represent the integrated phase noise from 1 MHz to 1 Hz. From our measurements, the suppression effect of phase noise of the unlocked $f_{\mathrm{b,amp}}$ (blue line in Fig. 5(a)) below 1 kHz becomes worse. Especially in the frequency offset range of 1 Hz-20 Hz, the noise increases in the form of $1/f^3$. This noise is largely contributed by the tens of meters of fiber and free-space path in the stretcher, amplifier, and compressor. Temperature fluctuation and mechanical vibration change the length of these optical paths. Furthermore, different from the ordinary multi-branch optical comb by shortening the non-common mode optical interferometer paths, high power amplifier optical paths cannot

Optics EXPRESS

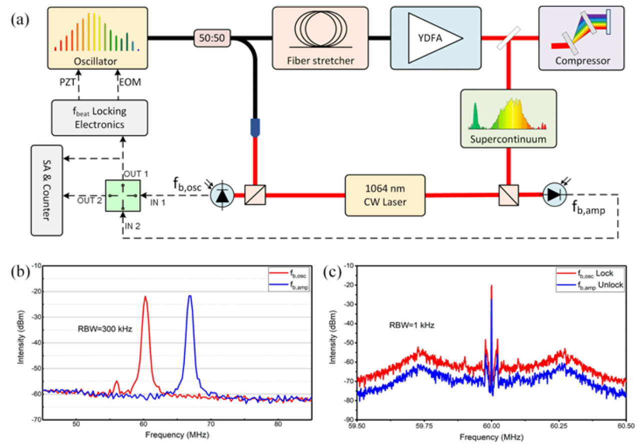

Fig. 4. (a) Schematic diagram of two locking methods of optical frequency comb locking to optical reference, YDFA: Yb-doped fiber amplifier; $f_{\mathrm{b,osc}}$: beat note of oscillator output with CW laser, $f_{\mathrm{b,amp}}$: beat note of amplifier output with CW laser. SA: spectrum analyzer. (b) RF spectra of $f_{\mathrm{b,osc}}$ (red) and $f_{\mathrm{b,amp}}$ (blue). (c) RF spectra of the locked $f_{\mathrm{b,osc}}$ signal and unlocked $f_{\mathrm{b,amp}}$ signal.

be reduced to the order of meters-level, and even need to be further increased in higher power optical comb. Fortunately, this noise can be eliminated by directly locking the amplifier branch to optical reference. When the $f_{\mathrm{b,amp}}$ is locked, the noise within 270 kHz (closed-loop bandwidth), corresponding to the servo bump in Fig. 4(c), is effectively suppressed.

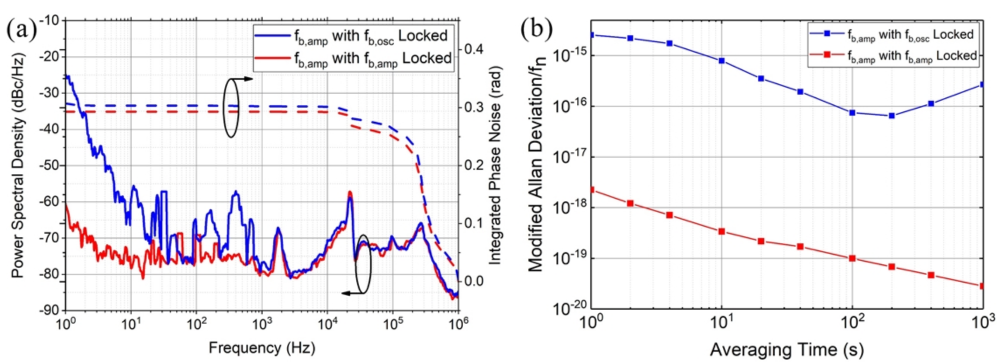

Fig. 5. (a) The noise power spectral density and integrated phase noise of $f_{\mathrm{b,amp}}$ in two different locking states. (b) The modified Allan deviation of $f_{\mathrm{b,amp}}$ in two different locking states.

Due to the increasing low-frequency noise of the unlocked branch, we further explored the long-term instability of $f_{\mathrm{b,amp}}$ in different locked states. Figure 5(b) shows the Allan variance of $f_{\mathrm{b,amp}}$ signals. When the oscillator branch is locked and the amplifier branch is unlocked, the instability of $f_{\mathrm{b,amp}}$ at 1 s is about 1.5×10^{-15}, and it drops to 9×10^{-17} at 100 s. Especially at gate time larger than 100 s, the Allan variance curve begins to bend upward with time, which indicates that there is a frequency drift on this time scale. In the amplifier system, the long-term thermal effect accumulated causes such frequency drift of the unlocked branches. When the amplifier branch is locked, the frequency instability of $f_{\mathrm{b,amp}}$ at 1 s gate time is about 2×10^{-18}

and drops to 3×10^{-20} at 1000 s. This result suggests that the long-term noise induced by the environmental fluctuations also can be suppressed by the feedback loop.

The white phase noise induced by ASE in the amplifier, amplitude-to-phase coupling caused by pump relative intensity noise, and spectral coherence deterioration in supercontinuum generation mainly reduced high-frequency stability. But in the high-frequency range of more than 1 kHz in Fig. 5(a), the $f_{\mathrm{b,amp}}$ has the same noise characteristics in different locked states. The integrated phase noise (IPN) of two locked states is 293 mrad (red dotted line in Fig. 5(a)) and 307 mrad (blue dotted line in Fig. 5(a)), respectively. This small difference in IPN between these two locked states shows that the noise control techniques, i.e., LMA-PCF in amplifier and tapered PCF in supercontinuum generation, are effective.

3.2. Out-of-loop instability measurement with two high-power combs

To fully characterize the out-of-loop frequency instability of the high-power OFC, we built two identical high-power optical frequency comb systems locked to one ultrastable CW laser. The out-of-loop instability is characterized by measuring the beat note of two combs. This measurement method can provide the real absolute instability of the comb which is not limited by the reference laser stability. Figure 6(a) shows two combs that have the same repetition rates and different offset frequencies in the frequency domain. We locked two optical combs on the same 1064 nm stabilized CW laser. Figure 6(b) shows the diagram of out-of-loop instability measurement with two fully locked high-power combs. The pulse after the amplifier and compression is divided into two branches. One of the branches broadens the spectrum in PCF and then divides into two channels to obtain f_{ceo} and f_{beat} respectively. The $f_{\mathrm{ceo},1}$, $f_{\mathrm{beat},1}$, $f_{\mathrm{ceo},2}$ and $f_{\mathrm{beat},2}$ measured here are in-loop frequency instabilities. The other branch is the application branch with an output power of 20 W. The out-of-loop non-collinear optical path is less than 1 m, and especially, to maintain the same non-collinear noise, the two optical paths from the two combs need to keep the same length, all less than 1 m. All frequency synthesizers and counters in the system are synchronized to the same reference clock. The overlap of pulses from two combs is achieved by slightly changing the RF reference of one of the optical combs when locking. The SNR of the out-of-loop f_{beat} signal is 60 dB at 500 kHz RBW. The phase noise characteristics and frequency instability of f_{beat} are measured by a spectrum analyzer and frequency counter.

Figure 7(a) shows the phase noise power spectral density (solid lines) and integrated phase noise (dashed lines) of $f_{\mathrm{beat},1}$, $f_{\mathrm{beat},2}$, and f_{beat}. As $f_{\mathrm{beat},1}$, $f_{\mathrm{beat},2}$ are locked by two different PLL circuits, their noise performance is also different. The integrated phase noise of these two beat notes is 293 mrad and 67 mrad respectively. The IPN of out-of-loop f_{beat} is 800 mrad. Figure 7(b) shows the in-loop frequency instability of beat notes of the two optical frequency combs, and the out-of-loop frequency stability between the two optical combs. The in-loop frequency instability can reach 2×10^{-18}/s at 282 THz. The frequency stability of the beat frequency signal outside the loop is 4.4×10^{-17}/s and drops to 6.5×10^{-19}/1000 s at 288 THz. We assume that the noise contributions of the two combs are uncorrelated and equal. The average instability to a single comb is 3.1×10^{-17}. This result is the best out-of-loop comparison result at present and has reached the level of the best optical atomic clock [43].

The amplifier and in-loop heterodyne beat are all integrated into a single aluminum housing for good packaging, which greatly reduces the impact of environmental fluctuation. For the housing structure limitation, we didn't measure the out-of-loop stability of the supercontinuum branch. However, since the supercontinuum branch is closer to the in-loop locking point, its frequency stability will be better than that of the amplifier branch. Since the CEO's instability reflects the relative stability of the two comb lines across the octave, the lower limit of the stability offset from the reference frequency is the CEO's stability.

The out-of-loop heterodyne optical path is the major factor affecting the frequency instability. We try to use a 5 m optical path, corresponding to the out-of-loop frequency instability of

Optics EXPRESS

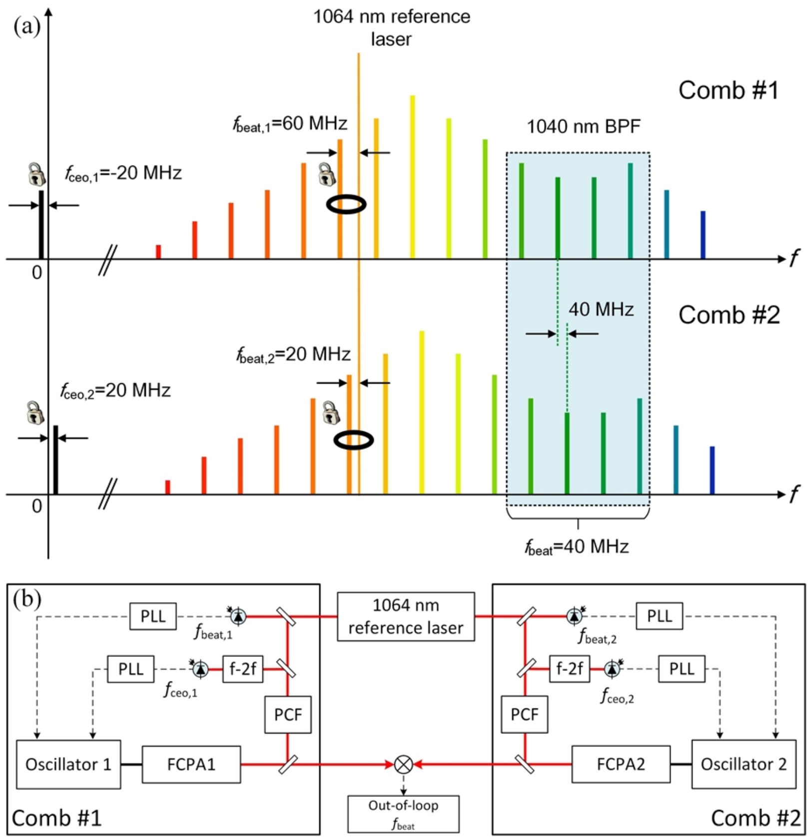

Fig. 6. Experimental set-up of out-of-loop instability measurement. (a) Two combs locked to the same stabilized 1064 nm optical reference with the same repetition rates and different offset frequencies in the frequency domain. The $f_{ceo,1}$ and $f_{beat,2}$ are locked to -20 MHz and 60 MHz respectively, and $f_{ceo,2}$ and f_{beat} are locked to 20 MHz and 20 MHz respectively. The out-of-loop beat f_{beat} is 40 MHz. (b) The diagram of out-of-loop instability measurement between two fully locked high-power combs. FCPA: fiber chirped pulsed amplifier.

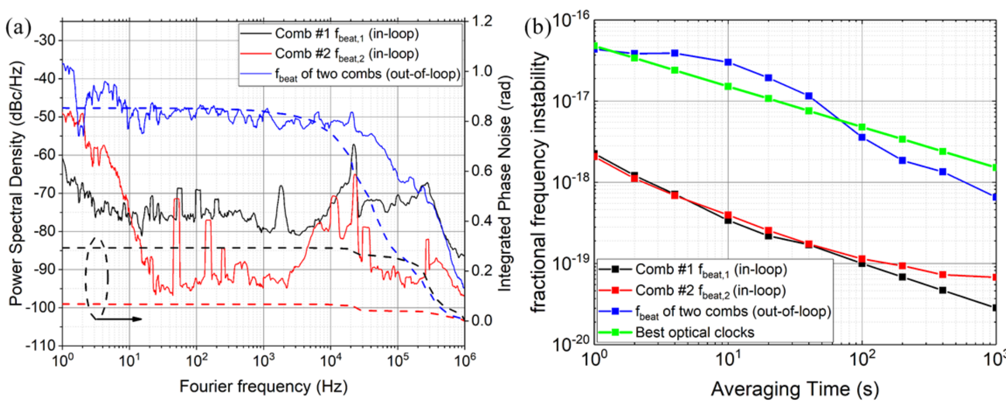

Fig. 7. Phase noise and fractional frequency instability of the in-loop and out-of-loop beat note. (a) Phase noise power spectral density of $f_{beat,1}$, $f_{beat,2}$ and out-of-loop f_{beat} of two combs. The dashed line represents the integrated phase noise from 1 Hz-1 MHz. (b) The modified Allan deviation of $f_{beat,1}$, $f_{beat,2}$ and out-of-loop f_{beat}.

5×10^{-16}/s, which is one order of magnitude larger than that at 1 m in Fig. 7 (b). The other important factor is the beat note SNR. For a 1 m optical path, the instability is different when the SNR is 40 dB and 60 dB at 500 kHz RBW. See Supplement 1 for more details.

4. Conclusions

In this study, we made a high-power optical frequency comb system based on an NPE mode-locked Yb-fiber oscillator and a linear LMA Yb-PCF CPA amplifier. To achieve low noise femtosecond laser pulse performance, single-mode fiber and high-order dispersion compensation fiber are used to stretch the pulse duration and pre-compensated the second-order and third-order dispersion caused by the fiber amplification of the system. By compression with a pair of high-efficiency grating, 75 fs laser pulses without double-base tailing are obtained with a power of more than 20 W. With the wideband phase-locked loop electronics, the high power frequency comb is locked to the ultrastable CW laser at 1064 nm. The f_{ceo} signal with a signal-to-noise ratio of 37 dB is phase-locked to the microwave reference and the instability at the optical carrier frequency is 2.9×10^{-19} in 1000 s. We further focused on the noise and frequency stability characteristics of 20 W comb output when locking either the oscillator branch or amplifier branch to the CW optical reference. The measurement results show that when the oscillator branch is locked, the environmental noise of the low-frequency cannot be compensated by the feedback loop, so it will seriously affect the amplifier output in long-term frequency stability, it's only 2.7×10^{-16} at 1000 s; when the amplifier branch is locked, the amplifier output has the lowest noise and the highest frequency stability, the instability of amplifier output is 2.8×10^{-20} at 1000 s. So, we can conclude that only by locking the amplifier branch, the comb can maintain the same instability as the ultrastable laser.

The state-of-the-art high power frequency comb with more than 20 W and 10^{-19} instability in 1000 s would see a wide perspective in the future. In addition to the extreme ultraviolet frequency comb generation and nonlinear ultraviolet optical spectroscopy [13], long-distance time and frequency transfer via dual-comb technology between earth-to-earth, satellite-to-earth and satellite-to-satellite are in growing demand. Taking the satellite-to-earth transfer with a distance of about 30,000 km as an example, the loss caused by the atmospheric absorption and scattering is up to 80 dB, so 20 W high power frequency combs would be necessary in this case [11]. We will continue optimizing and engineering the 20 W laser frequency comb and make it work well in the future space-earth integration time and frequency transfer network.

Funding. The Strategic Priority Research Program of the Chinese Academy of Sciences (XDA1502040404, XDB2101040004); National Natural Science Foundation of China (11078022, 60808007, 61378040, 91850209).

Disclosures. The authors declare no conflicts of interest.

Data availability. The original contributions presented in the study are included in the article/supplementary material, further inquiries can be directed to the corresponding author.

Supplemental document. See Supplement 1 for supporting content.

References

1. S. A. Diddams, T. Udem, J. C. Bergquist, E. A. Curtis, R. E. Drullinger, L. Hollberg, W. M. Itano, W. D. Lee, C. W. Oates, K. R. Vogel, and D. J. Wineland, "An Optical Clock Based on a Single Trapped 199 Hg + Ion," Science **293**(5531), 825–828 (2001).
2. A. D. Ludlow, M. M. Boyd, J. Ye, E. Peik, and P. O. Schmidt, "Optical atomic clocks," Rev. Mod. Phys. **87**(2), 637–701 (2015).
3. T. Nakamura, J. Davila-Rodriguez, H. Leopardi, J. A. Sherman, T. M. Fortier, X. J. Xie, J. C. Campbell, W. F. McGrew, X. G. Zhang, Y. S. Hassan, D. Nicolodi, K. Beloy, A. D. Ludlow, S. A. Diddams, and F. Quinlan, "Coherent optical clock down-conversion for microwave frequencies with 10(-18) instability," Science **368**(6493), 889–892 (2020).
4. F. Krausz and M. Ivanov, "Attosecond physics," Rev. Mod. Phys. **81**(1), 163–234 (2009).
5. T. Rosenband, D. B. Hume, P. O. Schmidt, C. W. Chou, A. Brusch, L. Lorini, W. H. Oskay, R. E. Drullinger, T. M. Fortier, J. E. Stalnaker, S. A. Diddams, W. C. Swann, N. R. Newbury, W. M. Itano, D. J. Wineland, and J. C.

Optics EXPRESS

Bergquist, "Frequency ratio of Al+ and Hg+ single-ion optical clocks; Metrology at the 17th decimal place," Science **319**(5871), 1808–1812 (2008).
6. I. Coddington, W. C. Swann, L. Nenadovic, and N. R. Newbury, "Rapid and precise absolute distance measurements at long range," Nat. Photonics **3**(6), 351–356 (2009).
7. M. T. Murphy, T. Udem, R. Holzwarth, A. Sizmann, L. Pasquini, C. Araujo-Hauck, H. Dekker, S. D'Odorico, M. Fischer, T. W. Hansch, and A. Manescau, "High-precision wavelength calibration of astronomical spectrographs with laser frequency combs," Mon. Not. Roy. Astron. Soc. **380**(2), 839–847 (2007).
8. I. Coddington, N. Newbury, and W. Swann, "Dual-comb spectroscopy," Optica **3**(4), 414–426 (2016).
9. X. P. Xie, R. Bouchand, D. Nicolodi, M. Giunta, W. Hansel, M. Lezius, A. Joshi, S. Datta, C. Alexandre, M. Lours, P. A. Tremblin, G. Santarelli, R. Holzwarth, and Y. Le Coq, "Photonic microwave signals with zeptosecond-level absolute timing noise," Nat. Photonics **11**(1), 44–47 (2017).
10. F. R. Giorgetta, W. C. Swann, L. C. Sinclair, E. Baumann, I. Coddington, and N. R. Newbury, "Optical two-way time and frequency transfer over free space," Nat. Photonics **7**(6), 434–438 (2013).
11. Q. Shen, J. Y. Guan, T. Zeng, Q. M. Lu, L. Huang, Y. Cao, J. P. Chen, T. Q. Tao, J. C. Wu, L. Hou, S. K. Liao, J. G. Ren, J. Yin, J. J. Jia, H. F. Jiang, C. Z. Peng, Q. Zhang, and J. W. Pan, "Experimental simulation of time and frequency transfer via an optical satellite-ground link at 10(-18) instability," Optica **8**(4), 471–476 (2021).
12. Q. Shen, J.-Y. Guan, J.-G. Ren, T. Zeng, L. Hou, M. Li, Y. Cao, J.-J. Han, M.-Z. Lian, and Y.-W. Chen, "Free-space dissemination of time and frequency with 10− 19 instability over 113 km," Nature **610**(7933), 661–666 (2022).
13. A. Cingoz, D. C. Yost, T. K. Allison, A. Ruehl, M. E. Fermann, I. Hartl, and J. Ye, "Direct frequency comb spectroscopy in the extreme ultraviolet," Nature **482**(7383), 68–71 (2012).
14. B. Seiferle, L. von der Wense, P. V. Bilous, I. Amersdorffer, C. Lemell, F. Libisch, S. Stellmer, T. Schumm, C. E. Düllmann, and A. Pálffy, "Energy of the 229Th nuclear clock transition," Nature **573**(7773), 243–246 (2019).
15. R. Paschotta, J. Nilsson, A. C. Tropper, and D. C. Hanna, "Ytterbium-doped fiber amplifiers," IEEE J. Quantum Electron. **33**(7), 1049–1056 (1997).
16. N. Mortensen, M. D. Nielsen, J. R. Folkenberg, A. Petersson, and H. R. Simonsen, "Improved large-mode-area endlessly single-mode photonic crystal fibers," Opt. Lett. **28**(6), 393–395 (2003).
17. J. Limpert, F. Roser, D. N. Schimpf, E. Seise, T. Eidam, S. Hadrich, J. Rothhardt, C. J. Misas, and A. Tunnermann, "High Repetition Rate Gigawatt Peak Power Fiber Laser-Systems: Challenges, Design, and Experiment," IEEE J. Sel. Top. Quantum Electron. **15**(1), 159–169 (2009).
18. A. Ruehl, A. Marcinkevicius, M. E. Fermann, and I. Hartl, "80 W, 120 fs Yb-fiber frequency comb," Opt. Lett. **35**(18), 3015–3017 (2010).
19. X. L. Li, M. A. R. Reber, C. Corder, Y. N. Chen, P. Zhao, and T. K. Allison, "High-power ultrafast Yb: fiber laser frequency combs using commercially available components and basic fiber tools," Rev. Sci. Instrum. **87**(9), 14 (2016).
20. D. P. Luo, Y. Liu, C. L. Gu, Z. W. Zhu, Z. J. Deng, L. Zhou, Y. F. Di, G. H. Xie, and W. X. Li, "130 W, 180 fs ultrafast Yb-doped fiber frequency comb based on chirped-pulse fiber amplification," Opt. Express **28**(4), 4817–4824 (2020).
21. D. P. Luo, Y. Liu, C. L. Gu, C. Wang, Z. W. Zhu, W. C. Zhang, Z. J. Deng, L. Zhou, W. X. Li, and H. P. Zeng, "High-power Yb-fiber comb based on pre-chirped-management self-similar amplification," Appl. Phys. Lett. **112**(6), 5 (2018).
22. A. Klenke, M. Müller, H. Stark, M. Kienel, C. Jauregui, A. Tünnermann, and J. Limpert, "Coherent beam combination of ultrafast fiber lasers," IEEE J. Sel. Top. Quantum Electron. **24**(5), 1–9 (2018).
23. E. Shestaev, S. Hadrich, N. Walther, T. Eidam, A. Klenke, I. Seres, Z. Bengery, P. Jojart, Z. Varallyay, A. Borzsonyi, and J. Limpert, "Carrier-envelope offset stable, coherently combined ytterbium-doped fiber CPA delivering 1 kW of average power," Opt. Lett. **45**(23), 6350–6353 (2020).
24. B. A. C. O. N. B. Collaboration, "Frequency ratio measurements at 18-digit accuracy using an optical clock network," Nature **591**(7851), 564–569 (2021).
25. T. R. Schibli, I. Hartl, D. C. Yost, M. J. Martin, A. Marcinkevicius, M. E. Fermann, and J. Ye, "Optical frequency comb with submillihertz linewidth and more than 10 W average power," Nat. Photonics **2**(6), 355–359 (2008).
26. T. Nakamura, S. Tani, I. Ito, M. Endo, and Y. Kobayashi, "Piezo-electric transducer actuated mirror with a servo bandwidth beyond 500 kHz," Opt. Express **28**(11), 16118–16125 (2020).
27. T. Hellwig, S. Rieger, and C. Fallnich, "Toward an all-optically stabilized frequency comb based on a mode-locked fiber laser," Opt. Lett. **39**(3), 525–527 (2014).
28. D. D. Hudson, K. W. Holman, R. J. Jones, S. T. Cundiff, J. Ye, and D. J. Jones, "Mode-locked fiber laser frequency-controlled with an intracavity electro-optic modulator," Opt. Lett. **30**(21), 2948–2950 (2005).
29. H. A. Haus and A. Mecozzi, "Noise of mode-locked lasers," IEEE J. Quantum Electron. **29**(3), 983–996 (1993).
30. K. L. Corwin, N. R. Newbury, J. M. Dudley, S. Coen, S. A. Diddams, K. Weber, and R. Windeler, "Fundamental noise limitations to supercontinuum generation in microstructure fiber," Phys. Rev. Lett. **90**(11), 113904 (2003).
31. N. R. Newbury and W. C. Swann, "Low-noise fiber-laser frequency combs (Invited)," J. Opt. Soc. Am. B **24**(8), 1756–1770 (2007).
32. H. Leopardi, J. Davila-Rodriguez, F. Quinlan, J. Olson, J. A. Sherman, S. A. Diddams, and T. M. Fortier, "Single-branch Er:fiber frequency comb for precision optical metrology with 10(-18) fractional instability," Optica **4**(8), 879–885 (2017).
33. A. Rolland, P. Li, N. Kuse, J. Jiang, M. Cassinerio, C. Langrock, and M. E. Fermann, "Ultra-broadband dual-branch optical frequency comb with 10− 18 instability," Optica **5**(9), 1070–1077 (2018).

Optics EXPRESS

34. L.-S. Ma, Z. Bi, A. Bartels, L. Robertsson, M. Zucco, R. S. Windeler, G. Wilpers, C. Oates, L. Hollberg, and S. A. Diddams, "Optical frequency synthesis and comparison with uncertainty at the 10-19 level," Science **303**(5665), 1843–1845 (2004).
35. Y. Nakajima, H. Inaba, K. Hosaka, K. Minoshima, A. Onae, M. Yasuda, T. Kohno, S. Kawato, T. Kobayashi, T. Katsuyama, and F. L. Hong, "A multi-branch, fiber-based frequency comb with millihertz-level relative linewidths using an intra-cavity electro-optic modulator," Opt. Express **18**(2), 1667–1676 (2010).
36. K. Kashiwagi, Y. Nakajima, M. Wada, S. Okubo, and H. Inaba, "Multi-branch fiber comb with relative frequency uncertainty at 10− 20 using fiber noise difference cancellation," Opt. Express **26**(7), 8831–8840 (2018).
37. E. Benkler, B. Lipphardt, T. Puppe, R. Wilk, F. Rohde, and U. Sterr, "End-to-end topology for fiber comb based optical frequency transfer at the 10− 21 level," Opt. Express **27**(25), 36886–36902 (2019).
38. M. Giunta, W. Hänsel, M. Fischer, M. Lezius, T. Udem, and R. Holzwarth, "Real-time phase tracking for wide-band optical frequency measurements at the 20th decimal place," Nat. Photonics **14**(1), 44–49 (2020).
39. L. E. Nelson, D. Jones, K. Tamura, H. A. Haus, and E. Ippen, "Ultrashort-pulse fiber ring lasers," Appl. Phys. B: Lasers Opt. **65**(2), 277–294 (1997).
40. L. Nugent-Glandorf, T. A. Johnson, Y. Kobayashi, and S. A. Diddams, "Impact of dispersion on amplitude and frequency noise in a Yb-fiber laser comb," Opt. Lett. **36**(9), 1578–1580 (2011).
41. H.-B. Wang, H.-N. Han, Z.-Y. Zhang, X.-D. Shao, J.-F. Zhu, and Z.-Y. Wei, "An Yb-fiber frequency comb phase-locked to microwave standard and optical reference," Chin. Phys. B **29**(3), 030601 (2020).
42. X. Shao, H. Han, J. Ma, M. Zhang, and Z. Wei, "Impact of dispersion and intracavity polarization state on pump power fixed point in a Yb-fiber frequency comb," Front. Phys. **10**, 931 (2022).
43. E. Oelker, R. B. Hutson, C. J. Kennedy, L. Sonderhouse, T. Bothwell, A. Goban, D. Kedar, C. Sanner, J. M. Robinson, G. E. Marti, D. G. Matei, T. Legero, M. Giunta, R. Holzwarth, F. Riehle, U. Sterr, and J. Ye, "Demonstration of 4.8 x10(-17) stability at 1s for two independent optical clocks," Nat. Photonics **13**(10), 714–719 (2019).